Supporting Information

Mechanistic Framework for the Formation of Different Sulfur Species by Electron Irradiation of *n*-Dodecanethiol Self-Assembled Monolayers on Au(111) and Au(100)

Natalia D. Aagaard[†], Julio C. Azcárate[†,*], Jimena Olmos-Asar[‡], Marcelo M. Mariscal[‡], José Solla-Gullón[§], Eugenia Zelaya[†], Mariano H. Fonticelli[ǁ,*].

† Centro Atómico Bariloche (CAB), Comisión Nacional de Energía Atómica (CNEA) - CONICET, Av. Bustillo 9500, San Carlos de Bariloche, Río Negro R8402AGP, Argentina.

‡ Instituto de Investigaciones en Fisicoquímica de Córdoba (INFIQC) CONICET, Departamento de Química Teórica y Computacional, Facultad de Ciencias Químicas, Universidad Nacional de Córdoba, Córdoba, Argentina.

§ Institute of Electrochemistry, University of Alicante, Apdo. 99, E-03080 Alicante, Spain.

ǁ Instituto de Investigaciones Fisicoquímica Teóricas y Aplicadas (INIFTA), Departamento de Química, Facultad de Ciencias Exactas, Universidad Nacional de La Plata (UNLP) – CONICET, La Plata, Buenos Aires, Argentina.

1. Secondary electron generation

Radiation damage is mainly generated by secondary electrons that have energies lower than 50 eV. Figure S1 shows the normalized intensity of emitted electrons in the normal direction to the surface when the sample was irradiated by (a) X-rays from an Al Kα source (red spectrum) and (b) 600 eV electron beam (blue spectrum).

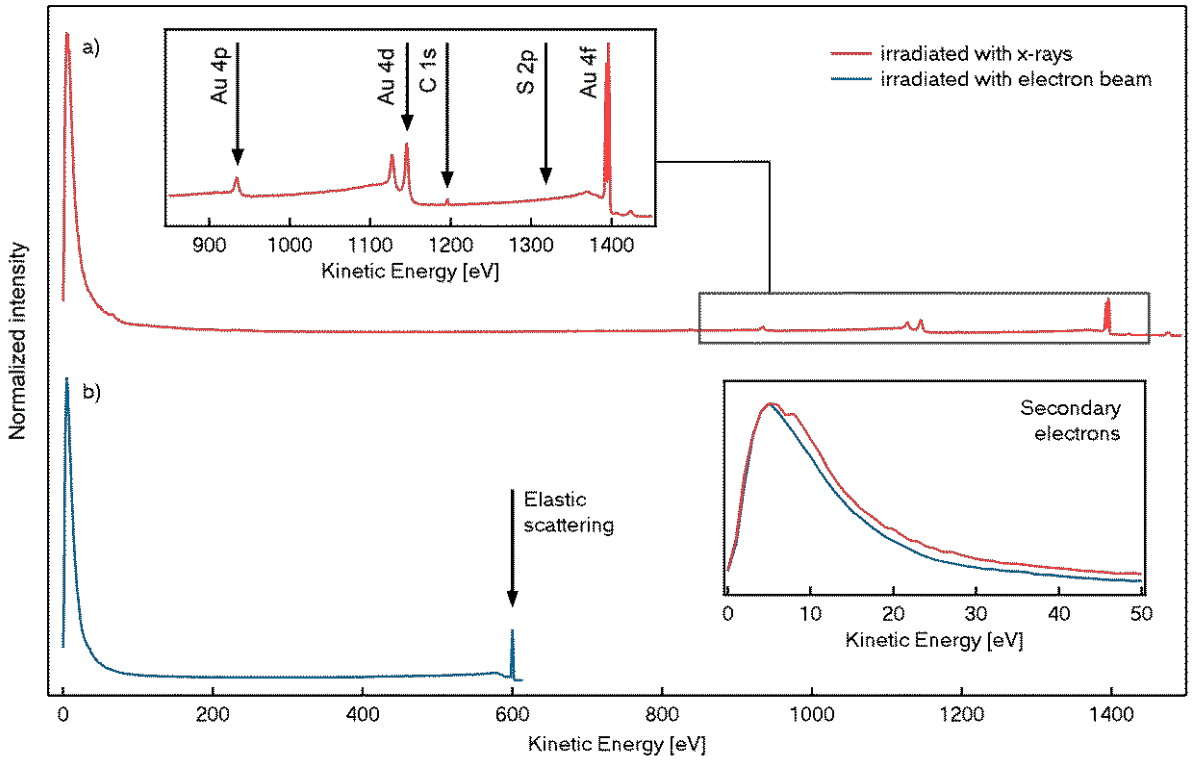

Figure S1: (a) normalized spectrum of emitted electrons when the sample was bombarded with X-rays from a source Al Kα. Relevant photoelectron signals are indicated by arrows in the upper inset. (b) normalized spectrum of emitted electrons when the sample was bombarded with 600 eV electrons at an incidence angle of 45º with respect to the surface normal. The bottom panel compares the normalized kinetic energy distribution for our experimental setting.

2. Comparison of the electron beam and X-ray damage

To induce damage in the SAMs we use a SPECS EQ 22/37 electron gun (described in the experimental section of the manuscript). It was set to generate 600 eV electrons and a current density (j) of 1 μA cm^{-2} (i ~0.25 μA in an irradiated area of 0.24 cm^2). Then, the accumulated dose of radiation can be calculated by the product of current density by irradiation time (t).

$$D = jt$$

In the case of X-ray irradiation during XPS measurement, the irradiated area is 10 mm^2 and a total photoelectron current of 7 pA was determined. According to the distribution of energy showed in the curve a) of figure S1, 41.2% of the emitted electrons have kinetic energies lower than 50 eV when the sample was irradiated with X-rays. In other words the coefficient of emission of secondary electrons is $\alpha = i_{\mathrm{SE}}/i_{\mathrm{PC}} = 0.41$. Then, we can calculate the secondary electron current density as:

$$j_{\mathrm{SE}} = \frac{i_{\mathrm{SE}}}{\mathrm{area}} = \frac{\alpha i_{\mathrm{PC}}}{\mathrm{area}} = 0.41\,\frac{7\ \mathrm{pA}}{10\ \mathrm{mm^2}} = 2.9 \times 10^{-5}\,\mu\mathrm{A\ cm^{-2}}$$

The XPS acquisition conditions were energy pass of 20 eV, energy step of 0.05 eV and dwell time of 0.1 s, with 40 scans between 168-159 eV for S 2p, 10 scans between 290-280 eV for C 1s and 5 scans between 94-80 eV (total irradiation time of 1065.5 s). Then, the total dose for each XPS measurement cycle is ~0.03 μC cm^{-2}.

In the case of incident electrons, we consider the secondary electron yield (SEY),[1,2] to avoid geometrical issues in the measurement and quantification of the reflected electrons (elastic scattering) in the energy distribution of curve b in figure S1. The SEY is the number of secondary electrons generated per each primary electron of higher energy. For Au surface, the SEY is ~1.6 at 600 eV.[2] Then, for the incident electron current density of 1 μA cm^{-2} the secondary electrons current density is 1.6 μA cm^{-2}. Finally, the dose of secondary electrons during one XPS acquisition cycle (0.03 μC cm^{-2}) would be attained by irradiation with 600 eV electrons in just ~0.02 s. For that reason the damage induced by X-ray irradiation can be neglected in comparison to that induced by the electron gun.

3. XP spectra evolution due to electron irradiation:

Figure S2 shows the C 1s XP spectra for pristine and damaged SAMs of dodecanethiolate on Au (100) and Au (111). It is clearly seen that the C 1s peaks for DDT-SAMs shift to lower BEs on Au (111) substrate. While on Au(100) substrate it exhibits a displacement to higher BEs at first, it decreases for higher doses.

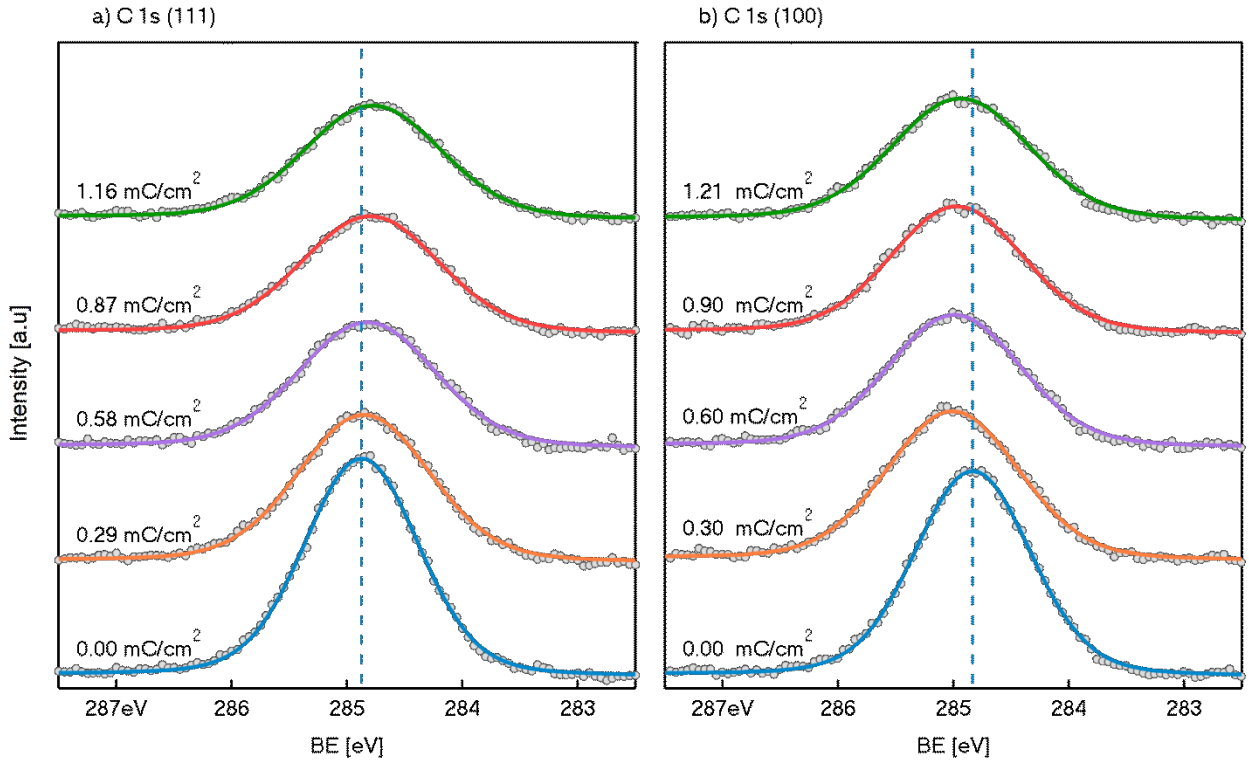

Figure S2: C 1s XP spectra for pristine (blue line) and damaged dodecanethiolate-SAMs on (a) Au (111) and (b) Au (100) at different irradiation dose.

In both SAMs, a decrease in intensity of C 1s signal is observed due to the loss of constituent material. This is consistent with an increase in the Au 4f signal due to decreased effect of attenuation phenomena (Figure S3).

The non-shift in the Au signal position along the irradiation process ensures that the changes observed in the C1s are not due to errors in the calibration of the BE scale.

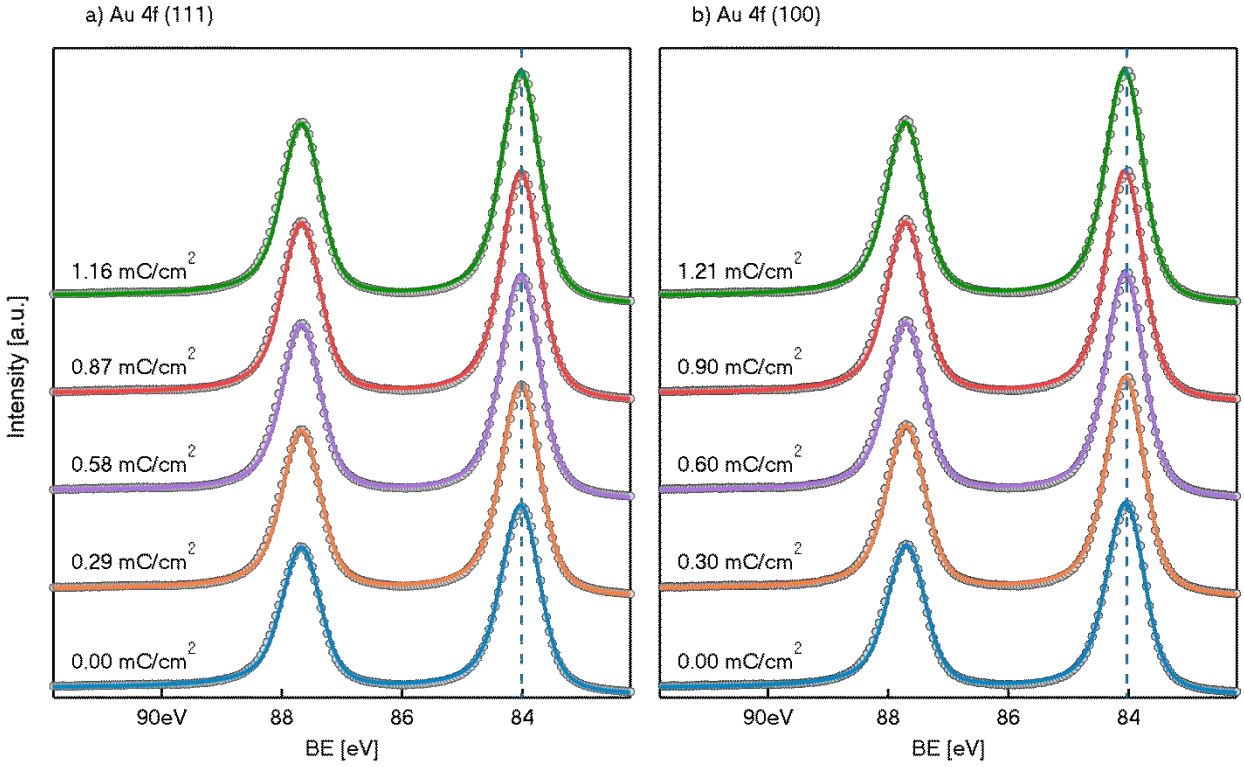

Figure S3: Au 4f XP spectra for pristine (blue line) and damaged dodecanethiolate -SAMs on (a) Au (111) and (b) Au (100) at different irradiation dose.

Figure S4 shows the evolution of the S 2p signal throughout the irradiation for both surfaces. These spectra, show a decrease in the area when doses increase. This is in concordance with the loss of material. The decrease in the thiolate signal, due to the cleavage of Au-S bond can be evidenced by the reduction of the $2p_{3/2}$ peak (S2). In addition, the increase in the relative abundance of damaged species is reflected in the growing of the S 2p signal at 163-164 eV (S3).

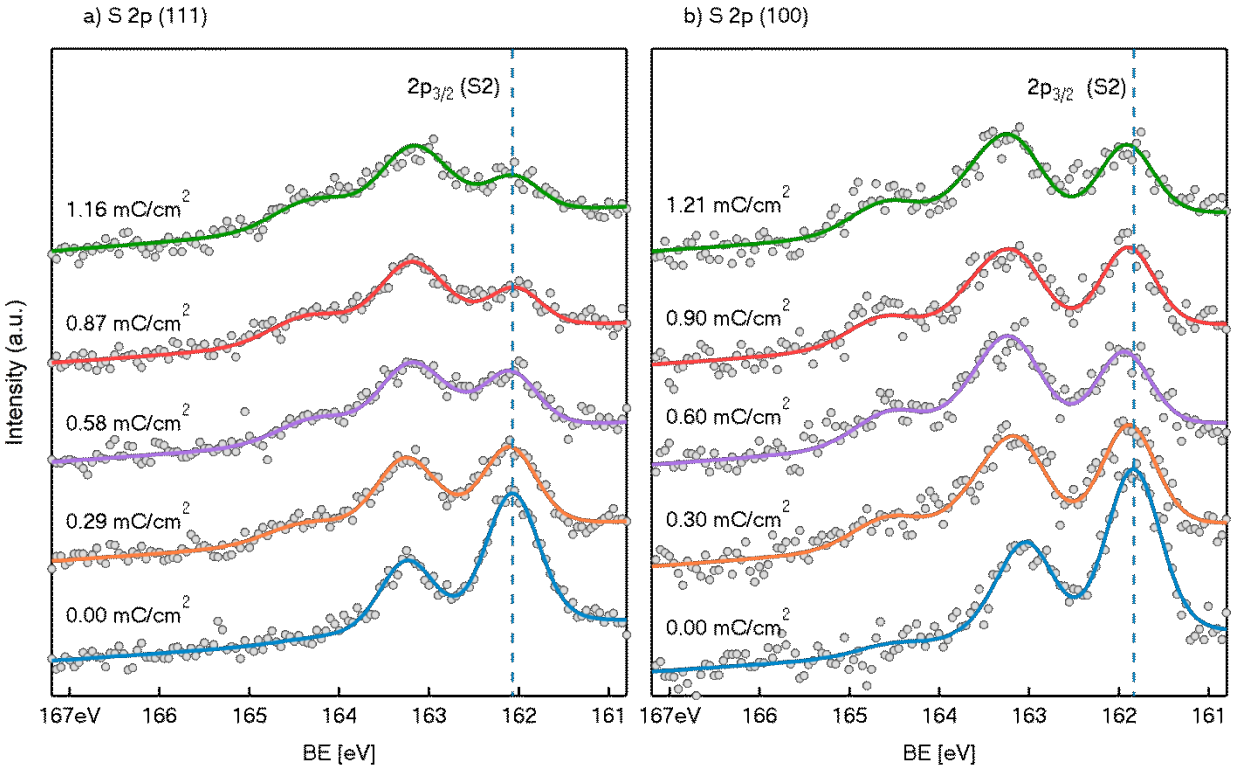

Figure S4: S 2p XP spectra for pristine (blue line) and damaged dodecanethiolate-SAMs on (a) Au (111) and (b) Au (100) at different irradiation dose.

4. Thiyl radical:

Figure S5a shows the density of states projected on sulfur orbitals for SCH_3 desorbed from Au(111). The most stable state has a total magnetization of 1, with an unoccupied p orbital. The unpaired spin is spatially localized on the sulfur atom, as shown in figure S5b.

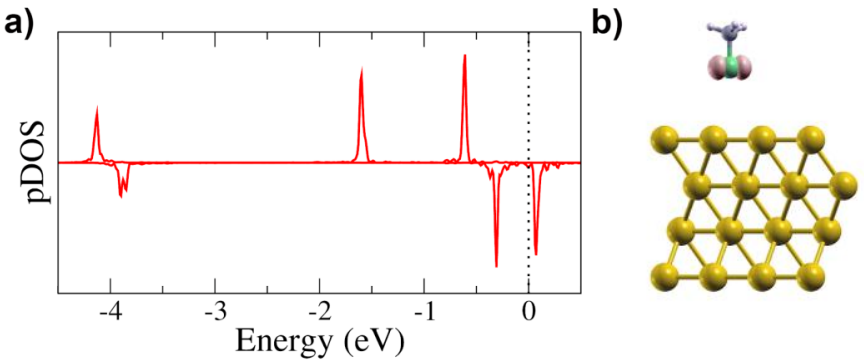

Figure S5: (a) Density of states projected on sulfur orbitals. The dotted line marks the Fermi Energy. (b) Spatial localization of the unpaired spin (in pink).

5. Reaction mechanisms initiated by RS^- and RS^+

The reactions initiated by RS^+ moieties could form either RS-R', RS-SR or RSH, as well as C=C. However, as C=C moieties must be consumed to form RS-R', this pathway cannot explain the presence of RS-R' and C=C in larger amounts on (111) than on (100) Au surfaces. In the case of reactions initiated by RS^- moieties it is not possible to form C=C (RS^- is a weak base, inefficient to withdraw an H^+ from an alkyl chain). Also, the reaction to form RS-R' would generates atomic sulfur (described as "S1" in the manuscript), which was neither found on Au(111) nor on Au(100) crystals (See Scheme S1).

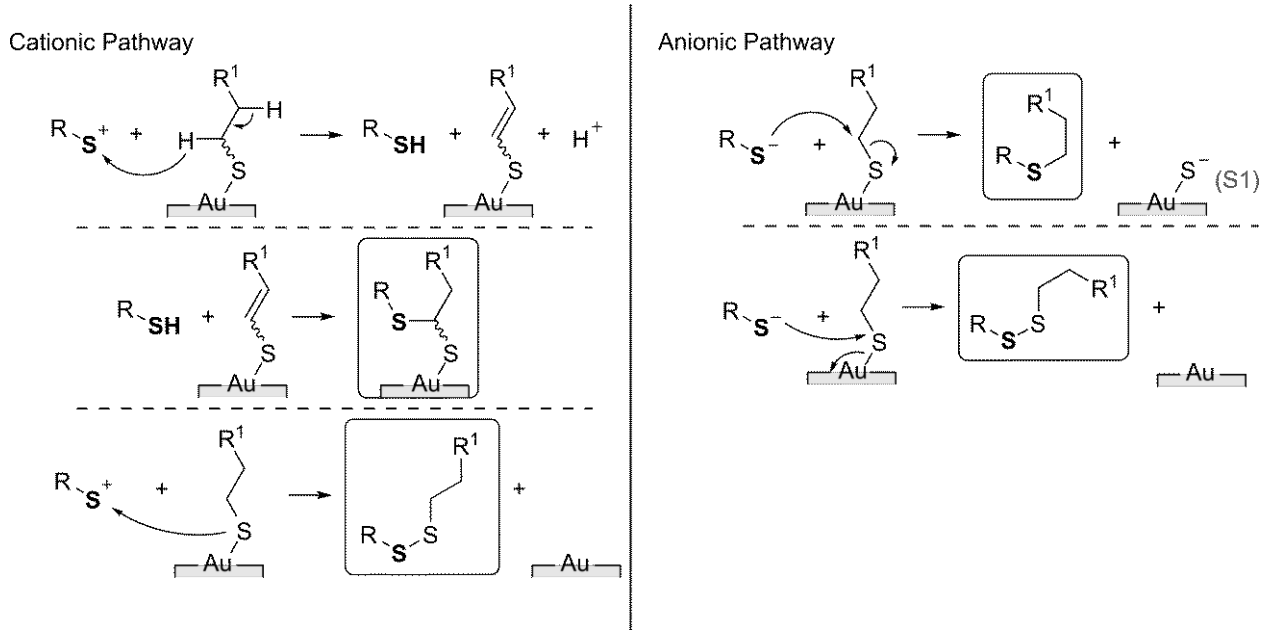

Scheme S1: Proposed reaction mechanism initiated by RS^+ (left) and RS^- (right).

REFERENCES

(1) Erdman, N.; Bell, D. C.; Reichelt, R. Scanning Electron Microscopy; 2019; pp 2–2.

(2) Gonzalez, L. A.; Angelucci, M.; Larciprete, R.; Cimino, R. The Secondary Electron Yield of Noble Metal Surfaces. *AIP Adv.* **2017**, *7* (11), 1–7.

Corresponding Author

* J.C.A. email: jcazcarate@cab.cnea.gov.ar, Ph: +54 294 444 5147, web: http://fisica.cab.cnea.gov.ar/metales

* M.H.F. email: mfonti@inifta.unlp.edu.ar, Ph: +54 221 425 7430, web: http://nano.quimica.unlp.edu.ar